

DIGITAL IMAGE ARTIFACTS RESTORATION

J. Ptáček¹, I. Šindelářová², and A. Procházka¹

¹ Institute of Chemical Technology, Department of Computing and Control Engineering

² University of Economics, Department of Econometrics

Abstract

The paper presents one of fundamental problems of digital image processing solving the task of the recovery of corrupted image regions. The first part of the paper is devoted to two dimensional interpolation using the iterative wavelet decomposition, thresholding and reconstruction. The second part presents the algorithm of the two dimensional interpolation using forward and backward prediction by signal model. The final part of the paper provides comparison of proposed algorithms.

1 Introduction

The paper is devoted to digital image enhancement, which falls within the generic multi-disciplinary area of information engineering, known as digital signal and image processing [7].

There are many applications in which signals are converted into a digital form and then digital signal processing methods are applied. In the case of digital image processing, the digital signal is two-dimensional. This work presents two different approaches for digital image enhancement problem. The main attention is paid to the digital image artifacts restoration.

The **recovery (restoration) of degraded parts (artifacts, blocks, regions)** of the digital image forms the main part of digital image enhancement. There are deterministic and probabilistic methods described in literature [3, 9] to solve this problem. The deterministic algorithms are usually based on autoregressive modelling, matrix moving average, or bilinear interpolation. Probabilistic methods include usually Bayesian modelling. Signals containing more random components can be more completely described by their probability distributions. Therefore Bayesian probabilistic methods are important in the analysis of two-dimensional signals. Iterated Wavelet Interpolation Method (IWIM) forms a new designed method to achieve this goal. This method is based on the interpolation using wavelet functions, i.e. the input image is decomposed by the selected wavelet function, treated in the wavelet domain, and then reconstructed back into the image with recovered corrupted or missing regions.

The methods described further have been developed and verified for simulated two-dimensional signals and then applied to processing of real biomedical images of the human brain obtained by the magnetic resonance method. All resulting algorithms are verified in the computational and visualization Matlab environment providing tools for remote signal processing using Matlab web server and computer network.

2 Principles of Discrete Wavelet Transform

Wavelet transforms (WT) provide an alternative to the short-time Fourier transform (STFT) for non-stationary signal analysis [2]. Both the STFT and the WT result in signal decomposition into two-dimensional function of time and frequency respectively scale. The basic difference between these two transforms is in the construction of the window function which has a constant length in the case of the STFT (including rectangular, Blackman and other window functions) while in the case of the WT wide windows are applied to low frequencies and short windows for high frequencies to ensure constant time-frequency resolution. Local and global signal analysis can be combined in this way. Wavelet functions used for signal analysis are derived from

the initial basic (mother) function forming the set of functions

$$W_{m,k}(t) = \frac{1}{\sqrt{a}} W\left(\frac{1}{a}(t-b)\right) = \frac{1}{\sqrt{2^m}} W(2^{-m}t - k) \quad (1)$$

for discrete parameters of dilation $a=2^m$ and translation $b=k2^m$. Wavelet dilation corresponds to the spectrum compression. The most common choice includes Daubechies wavelets even though their frequency characteristics stand for approximation of band-pass filters only. On the other hand harmonic wavelets introduced in [6] can have broader application in many engineering problems owing to their very attractive spectral properties.

3 Wavelet Decomposition and Reconstruction of Images

The principle of image wavelet decomposition [10] is presented in Fig. 1 for an image matrix $[G(n, m)]_{N,M}$. Any one-dimensional signal can be considered as a special case of an image having one column only.

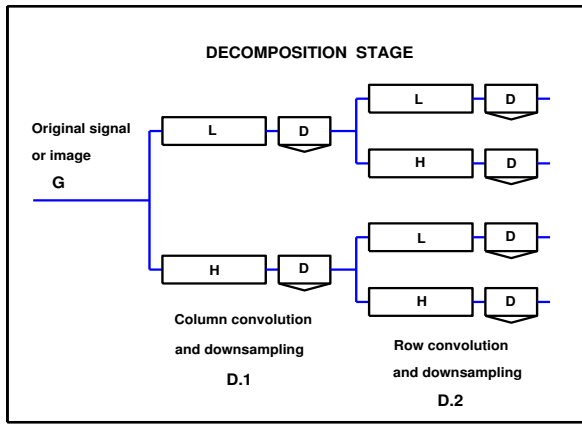


Figure 1: Principle of the 2-D wavelet decomposition followed by downsampling

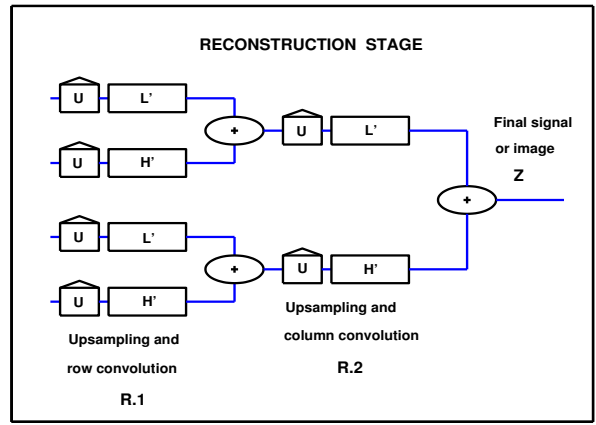


Figure 2: Principle of the backward 2-D wavelet reconstruction

The **decomposition stage** includes the processing of the image matrix by columns at first using wavelet (high-pass) and scaling (low-pass) function followed by row downsampling by factor D in stage $D.1$.

Let us denote a selected column of the image matrix $[G(n, m)]_{N,M}$ as signal $\{x(n)\}_{n=0}^{N-1} = [x(0), x(1), \dots, x(N-1)]^T$. This signal can be analyzed by a half-band low-pass filter represented by the scaling function with its impulse response

$$\{l(n)\}_{n=0}^{L-1} = [l(0), l(1), \dots, l(L-1)]^T \quad (2)$$

and corresponding high-pass filter represented by the wavelet function based upon impulse response

$$\{h(n)\}_{n=0}^{L-1} = [h(0), h(1), \dots, h(L-1)]^T \quad (3)$$

The first stage presented in Fig. 1 assumes the convolution of a given signal and the appropriate filter for decomposition at first by relations

$$d_0(n) = \sum_{k=0}^{L-1} l(k)x(n-k) \quad d_1(n) = \sum_{k=0}^{L-1} h(k)x(n-k) \quad (4)$$

for all values of n followed by subsampling by factor D . In the following decomposition stage $D.2$ the same process is applied to rows of the image matrix followed by row downsampling. The decomposition stage results in this way in four images representing all combinations of low-pass and high-pass initial image matrix processing.

The **reconstruction stage** shown in Fig. 2 includes row upsampling by factor U at first and row convolution in stage $R.1$. The corresponding images are then summed. The final step $R.2$ assumes column upsampling and convolution with reconstruction filters followed by summation of the results again.

In the case of one-dimensional signal processing, steps $D.2$ and $R.1$ are omitted. The whole process is called signal/image decomposition and perfect reconstruction using $D=2$ and $U=2$.

4 Image Artifacts Restoration Using Wavelet Transform

Image artifacts restoration represents a basic problem in image processing with many different applications including engineering, reconstruction of missing data during their transmission and enhancement of biomedical structures as well [11]. This problem occurs also in filling-in blocks of missing or corrupted data. The following method is based on the two-dimensional discrete wavelet transform approach. Iterated interpolation [4] based upon the wavelet transform forms the new method designed here. This method is verified for simulated data and then applied to processing of real magnetic resonance images. Sum of Squared Errors (SSE), Peak Signal-to-Noise Ratio (PSNR), and subjective aesthetic notion are the criteria of the consistency between the original image and image after the restoration.

We can view a sequence of lost samples as the result of a particular noise process acting on the original signal. However, unlike the traditional case, this noise process is not uncorrelated with the original signal. The designed method comes out from the signal wavelet denoising, which tries to keep transform coefficients of high PSNR while zeroing out coefficients having lower PSNR. Our primary assumption in this algorithm is that the transformation used to generate the wavelet transform coefficients mostly ensures that if vector \mathbf{c} is hard-thresholded to zero with $\delta \sim \sigma_e$, then with high probability $|\hat{\mathbf{c}}| \ll |e|$, i.e., hard-thresholding of \mathbf{c} removes more noise than signal by the following relation

$$\bar{c}(k) = \begin{cases} c(k) & \text{if } |c(k)| > \delta \\ 0 & \text{if } |c(k)| \leq \delta \end{cases} \quad (5)$$

where δ is a threshold limit, $\bar{\mathbf{c}}$ is a vector of thresholded coefficients, \mathbf{c} is a vector of wavelet coefficients of the signal containing an additive noise e , $\hat{\mathbf{c}}$ is a vector of wavelet coefficients of the signal without noise, and σ_e is a variance of noise.

The evaluation of the threshold limit δ is still in development process. It is possible to find some recommendations [1] for an estimation of δ , but precise analytic or empirical formula does not exist yet.

For digital biomedical images the following two approaches of a threshold limit estimation have been used:

- Global threshold limit $\delta = \sigma \sqrt{2 \ln(N \times M)}$, where σ is a variance of the wavelet transform coefficients in all decomposition branches, and $N \times M$ is the size of the processed image
- Threshold limit of an i -th branch $\delta_i = \sigma_i \sqrt{2 \ln(N \times M)}$ for $i = 1, 2, \dots, L$, where σ_i are variances of the wavelet transform coefficients in each decomposition branch i separately, and L is a number of wavelet decomposition branches

This algorithm makes changes just to the lost sequence of samples by the wavelet transform coefficients hard-thresholded to zero. When the value of the lost samples is changed, we can continue to evaluate these samples again. Input signal for the wavelet decomposition, hard-thresholding, and backward wavelet reconstruction, is a result of the previous iteration.

The algorithm is repeated until the SSE value between the restored and the original signal is acceptably low or required $PSNR$ value is achieved.

This proposed algorithm has been applied the real MR image of a human brain. Fig. 3 presents the wavelet decomposition of the original corrupted MR image (see Fig. 3(a)) into one decomposition level (Fig. 3(b)) using the Daubechies wavelet function of the 8th order. Fig. 3(d) shows the wavelet coefficients and modified, i.e. thresholded wavelet coefficients. Restored image (after the first iteration) can be seen in Fig. 3(c).

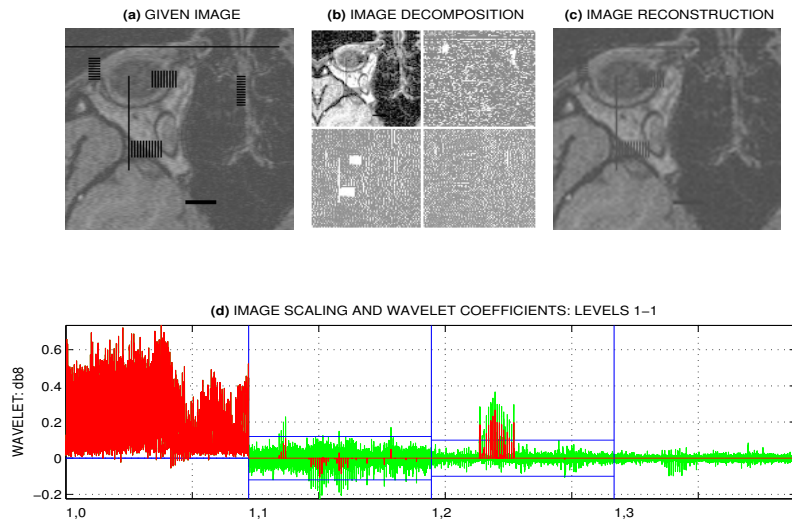


Figure 3: The first iteration of the real MR image restoration process presenting (a) given corrupted image, (b) image decomposition into one level, (c) backward wavelet reconstruction, and (d) wavelet, scaling coefficients

The final restored MR image with low acceptable SSE and high $PSNR$ has been obtained after 50 iterations of the iterative wavelet interpolation algorithm. Fig. 4(a) presents the original corrupted image and Fig. 4(b) restored image. Evolution of the $PSNR$ and SSE values during the whole restoration process is shown in Fig. 4(c),(d).

The best result of the MR image recovery has been obtained using the Daubechies wavelet function of the 8th order (see Table 1) for the wavelet decomposition into one level. Coefficients in the wavelet domain have been modified by the hard-thresholding method and reconstructed back to the real image.

Decomposition method (wavelet function)		PSNR1 [dB]	PSNR2 [dB]	SSE1	SSE2
1	<i>Haar</i>	32.0515	42.8529	15.1740	1.2617
2	<i>Daubechies of the 2nd order</i>		44.2262		0.9197
3	<i>Daubechies of the 4th order</i>		45.6256		0.6663
4	<i>Daubechies of the 8th order</i>		46.8670		0.5007
5	<i>Symmlet of the 2nd order</i>		44.2262		0.9197
6	<i>Symmlet of the 4th order</i>		45.7660		0.6451
7	<i>Symmlet of the 8th order</i>		46.4374		0.5527

Table 1: Peak Signal-to-Noise Ratio (PSNR) and Sum of Squared Errors (SSE) of the real MR image containing corrupted regions ($PSNR1$, $SSE1$) and the same MR image after the recovery process ($PSNR2$, $SSE2$) reconstructed by the selected wavelet functions after 350 iterations

This method is sufficient in the case of a limited number of interpolated pixels. If the corrupted block is large (it usually means more than 100 pixels), it is necessary to divide this region into more layers and to recover them step by step. Then the recovery algorithm starts by grouping the interpolated pixels (pixels in the lost block) into layers as shown in Fig. 5.

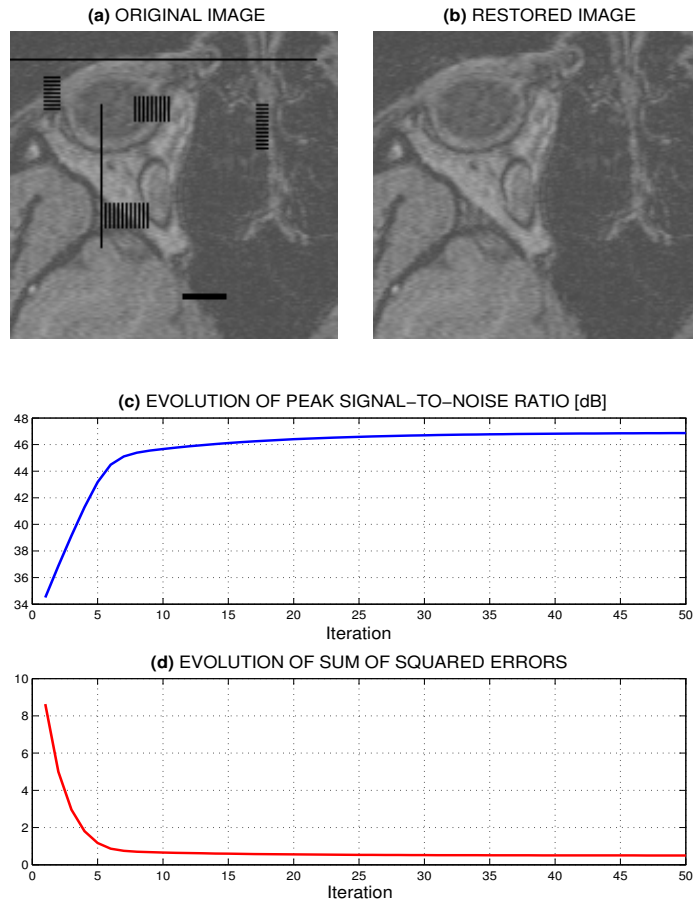


Figure 4: Restoration of the real MR image using the iterated wavelet interpolation method presenting (a) given corrupted image, (b) restored image (after 50 iterations), (c) evolution of the Peak Signal-to-Noise Ratio (PSNR) value, and (d) evolution of the Sum of Squared Errors (SSE) value during the iteration process

Layers are recovered in stages with each layer recovered by mainly using the information from the preceding layers, that is, layer 0 = image is used to recover layer 1, layers 0 and 1 are used to recover layer 2 etc. The layer grouping in Fig. 5 is of course one possibility, and many different groupings can be chosen depending on the size and shape of the lost blocks. Beyond the grouping into layers and associated recovery of layers in stages, the main steps of the algorithm amount to evaluating several complete transforms over the target layer, selective hard-thresholding of wavelet transform coefficients, inverse transforming to generate intermediate results, and finally clipping to obtain the recovered layer. Starting with an initial threshold δ_0 , these steps are carried out iteratively where at each iteration the threshold is evaluated again and the layers are recovered to finer detail using the new threshold. Prior to the first iteration, pixels in the lost block are assigned initial values, usually, the mean value computed from the surroundings of the outer boundary of layer 1.

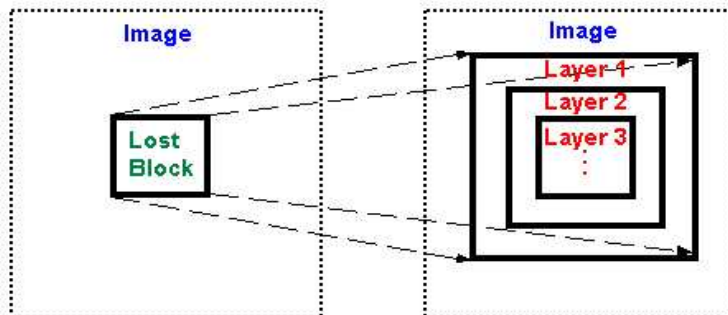


Figure 5: Layers of pixels in the recovery algorithm

```

% Name: iwim_MR
% Program Description: computes the real MR image recovery
% using the IWIM method, PSNR and SSE values
% Output: corrupted MR image, recovered image after 350
% iterations, PSNR and SSE values of the corrupted
% and recovered images, evolution of the PSNR and SSE
% values during the iterative calculation
% iteration process of the wavelet interpolation method
for i=1:350
    % threshold limits calculation
    [thr,sorh,keepapp] = ddencmp('den','wv',x);
    % wavelet decomposition, hard-thresholding,
    % and backward wavelet reconstruction using
    % the selected wavelet function
    [xd,CXC,LXC,PERF0,PERFL2] = wdencmp('gbl',x,'db8',1,thr,sorh,keepapp);
    % output is a new input in the next iteration
    x( XMASK)=xd( XMASK);
    % pixels value limitation
    xmask1=x>=0; x=x.*xmask1;
    xmask2=x>1; x=x.*(1-xmask2)+xmask2;
    % SSE and PSNR values evolution
    e(i)=sumsqr(x_noncorrupted-x);
    psnr_image(i)=psnr(x_noncorrupted,x);
end
% PSNR and SSE values
psnr_orig=psnr(x_noncorrupted,x_corrupted)
psnr_after=psnr(x_noncorrupted,x)
sse_orig=sumsqr(x_noncorrupted-x_corrupted)
sse_after=sumsqr(x_noncorrupted-x)

```

Figure 6: The main part of the Matlab program for image artifacts restoration using the iterative wavelet interpolation method

5 Image Artifacts Restoration Using Signal Modelling

Signal Modelling forms a quite different approach to image artifacts restoration than the 2-D transform methods. It is based upon forward and backward prediction by the autoregressive modelling applied to columns and rows in the neighbourhood of the reconstructed image area.

The predictive image modelling, also described in [5], uses an autoregressive method for the image blocks reconstruction. This algorithm forms the following steps:

- **Estimation of autoregressive parameters for signal prediction in each image row** using image values to the left and to the right of the corrupted block boundary
- **Estimation of autoregressive parameters for signal prediction in each image column** using image values to the top and to the bottom of the corrupted block boundary
- **Prediction of each pixel** inside the corrupted image block using models described in the previous steps and averaging of resulting values

The method is based upon prediction using an autoregressive (AR) model for forward prediction described by the following relation

$$z(m, i) = \sum_{j=1}^K a_j z(m, i-j) + u(m, i) \quad (6)$$

for $i = k+1, k+2, \dots$, where a_j are the AR parameters, K represents model order and $u(m, i)$ is the excitation including the model error.

Autoregressive model for backward prediction is defined as

$$z(m, i) = \sum_{j=1}^K b_j z(m, i+j) + u(m, i) \quad (7)$$

for $i = l-1, l-2, \dots$, where b_j are the AR parameters.

Construction of the autoregressive (AR) model is possible by the following algorithm. Consider a signal $\{x(i)\}_{i=1}^N$, where the successive M values starting with index l forming a sequence

$$\{x(l), x(l+1), \dots, x(l+M-1)\} \quad (8)$$

have been lost or corrupted.

In this case we try to use for the restoration of these samples forward and backward prediction using preceding samples and succeeding samples respectively. Let N_W and N_E be the number of samples on the left (west) and right (east) side of the missing segment to be used for the restoration of the signal. Then, the forward predicted signal $\hat{x}_W(i)$ is based on the samples

$$\{x(l-1), x(l-2), \dots, x(l-N_W)\} \quad (9)$$

and backward predicted signal $\hat{x}_E(i)$ on the samples

$$\{x(l+M), x(l+M+1), \dots, x(l+M+N_E-1)\} \quad (10)$$

This method uses both forward and backward prediction to achieve better results for the missing or corrupted segment of a signal. A condition of stationarity of a given signal is not necessary.

Construction of the AR models for 2-D signals is possible to find in [8]. Matlab code for image artifacts restoration using the autoregressive modelling of the signal can be seen in Fig. 7.

```

% Name: arm
% Program Description: Designs AR models for forward and backward prediction
% in horizontal and then in vertical direction, uses these
% models for an estimation of the missing image region
% Output: PSNR of the corrupted and recovered image, plot
% of the original, corrupted, and recovered image
% order of the AR model
Mh=M;Mv=M;kh=7;kv=7;nh=lh+Mh-1;nv=lv+Mv-1;km=170;
% horizontal direction
for j=1:Mv
    theta1=ar(X(lv+j-1,lh-km:lh-1)',kh,'fb'); % matrix A
    % vector of AR parameters in horizontal direction (forward prediction)
    a(j,:)=th2poly(theta1); a(j,:)=-a(j,:);
    aa(j,:)=[a(j,:) zeros(1,(Mh-size(a,2)))];
    r(j,:)=[-1 zeros(1,Mh-1)]; A(:,:,j)=toeplitz(aa(j,:),r(j,:));
    theta2=ar(X(lv+j-1,nh+km:-1:nh+1)',kh,'fb'); % matrix B
    % vector of AR parameters in horizontal direction (backward prediction)
    b(j,:)=th2poly(theta2); b(j,:)=-b(j,:); bb(j,:)=[b(j,:) ...
    zeros(1,(Mh-size(b,2)))];
    B(:,:,j)=toeplitz(r(j,:),bb(j,:));
...

```

```

% definition of matrix W (horizontal direction)
for i=1:kh
    W(i,:,j)=[zeros(1,i) X(lv+j-1,lh-1:-1:lh-1-kh+i)];
end
for i=kh+1:Mh; W(i,:,j)=zeros(1,kh+1); end
% definition of matrix E (horizontal direction)
for i=1:Mh-kh; E(i,:,j)=zeros(1,kh+1); end
for i=Mh-kh+1:Mh;
    E(i,:,j)=[zeros(1,Mh+1-i); X(lv+j-1,nh+1:nh+i-Mh+kh)];
end
end
% vertical direction
for j=1:Mh;
    theta3=ar(X(lv-km:lv-1,lh+j-1),kv,'fb'); % matrix C
% vector with AR parameters in vertical direction (forward prediction)
c(j,:)=th2poly(theta3); c(j,:)=-c(j,:); cc(j,:)=[c(j,:)
zeros(1,(Mv-size(c,2)))]]; r(j,:)=[-1 zeros(1,Mv-1)];
C(:,:,j)=toeplitz(cc(j,:),r(j,:));
theta4=ar(X(nv+km:-1:nv+1,lh+j-1),kv,'fb'); % matrix D
% vector with AR parameters in vertical direction (backward prediction)
d(j,:)=th2poly(theta4); d(j,:)=-d(j,:); dd(j,:)=[d(j,:)
zeros(1,(Mv-size(d,2)))]]; D(:,:,j)=toeplitz(r(j,:),dd(j,:));
% definition of matrix S (vertical direction)
for i=1:kv
    S(i,:,j)=[zeros(1,i) X(lv-1:-1:lv-1-kv+i,lh+j-1)'];
end
for i=kv+1:Mv; S(i,:,j)=zeros(1,kv+1); end
% definition of matrix N (vertical direction)
for i=1:Mv-kv; N(i,:,j)=zeros(1,kv+1); end
for i=Mv-kv+1:Mv
    N(i,:,j)=[zeros(1,Mv+1-i); X(nv+1:nv+i-Mv+kv,lh+j-1)'];
end
end
% calculation of G and Y matrices
for j=1:Mh
    G1(:,:,j)=A(:,:,j)'*A(:,:,j)+B(:,:,j)'*B(:,:,j);
    G2(:,:,j)=C(:,:,j)'*C(:,:,j)+D(:,:,j)'*D(:,:,j);
    y1=-A(:,:,j)'*W(:,:,j)*a(j,:)'-B(:,:,j)'*E(:,:,j)*b(j,:)' ;
    y2=-C(:,:,j)'*S(:,:,j)*c(j,:)'-D(:,:,j)'*N(:,:,j)*d(j,:)' ;
    XXn1(j,:)=y1'*inv(G1(:,:,j));
    XXn2(j,:)=y2'*inv(G2(:,:,j));
end
XXn2=XXn2';
% arithmetic mean of the interpolation in horizontal and vert. directions
XXn=(XXn1+XXn2)./2;
% restoration of the corrupted image
Xr=X; Xr(lv:lv+M-1,lh:lh+M-1)=XXn;Mn=101;

```

Figure 7: The main part of the Matlab program for image artifacts restoration using the AR modelling of the signal

6 Results and Conclusions

Each method has its advantages for the recovery of specific image artifacts or replacement of image missing parts. To compare two designed methods described above in practical usage, one corrupted region of the MR image has been restored using designed algorithms. Table 2 presents an evaluation of the restoration process using the *PSNR* and *SSE* values. This table can look upon from the point of view of an objective criteria of the restoration evaluation. Another point of view forms a subjective aesthetical notion of specialists in the appropriate field. In the case of MR images the restoration results have been discussed with doctors of the Královské Vinohrady hospital in Prague.

Recovery Method		PSNR1 [dB]	PSNR2 [dB]	SSE1	SSE2
1	<i>Autoregressive Modelling</i>	44.28	52.83	8.5528	0.0532
2	<i>Matrix Moving Average</i>		52.14		0.0613
3	<i>Bilinear Interpolation</i>		50.41		0.4258
5	<i>Bayesian Modelling</i>		52.83		0.0541
7	<i>Autoregressive Modelling after the Wavelet Decomposition</i>		52.94		0.0537
9	<i>Iterated Wavelet Interpolation</i>		53.30		0.0526

Table 2: Comparison of selected designed image restoration methods including Peak Signal-to-Noise-Ratio (PSNR) and Sum of Squared Errors (SSE) of the real MR image containing one corrupted region (*PSNR1*, *SSE1*) and the restored MR image using selected restoration methods (*PSNR2*, *SSE2*)

Simple methods based upon a limited region of interest are very fast and easy to implement but they provide good results for a restoration of low-frequency components only. In the case we need to restore images of higher frequency components, it is useful to apply more complicated linear, nonlinear or statistical models both in the original image domain or after the application of the appropriate transform functions.

Each 2-D signal requires a different approach for its processing according to its features, therefore it is difficult to decide, which algorithm is more applicable for digital images restoration even we have images of one sort (in this case MR images). The success of restoration and the choice of restoration method depend on:

- **The sort** of digital images
- **The character of signal components** contained in the image (periodical, random)
- **The size** of the corrupted region
- **The shape** of the corrupted region
- **The character of signal components in the surrounding** of the corrupted region

The right choice and usage of the restoration algorithm should respect all the points mentioned above to get the best digital image regions restoration.

Acknowledgments

The work has been supported by the research grant of the Faculty of Chemical Engineering of the Institute of Chemical Technology, Prague No. MSM 223400007. All real MR images have been kindly provided by the Královské Vinohrady Faculty Hospital in Prague.

References

- [1] A. Bruce, D. Donoho, and Hong-Ye Gao. Wavelet Analysis. *IEEE Spectrum*, 33(10):26–35, October 1996.
- [2] L. Debnath. *Wavelets and Signal Processing*. Birkhauser Boston, Boston, U.S.A., 2003.
- [3] A. Duci, A. J. Yezzi, S. K. Mitter, and S. Soatto. Region Matching with Missing Parts. In *7th European Conference on Computer Vision-Part III, pages: 48-64, London, U.K.* Springer-Verlag, 2002.
- [4] Onur G. Guleryuz. Iterated Denoising for Image Recovery. In *Data Compression Conference (DCC '02), Snao Bird, Utah*. IEEE, 2002.
- [5] B. W. Hwang and S. W. Lee. Reconstruction of Partially Damaged Face Images Based on a Morphable Face Model. *IEEE Transactions on Pattern Analysis and Machine Intelligence*, 4(5):365–372, 2003.
- [6] D. E. Newland. *An Introduction to Random Vibrations, Spectral and Wavelet Analysis*. Longman Scientific & Technical, Essex, U.K., third edition, 1994.
- [7] I. Pitas. *Digital Image Processing Algorithms and Applications*. John Wiley & Sons, Inc., New York, 2000.
- [8] J. Ptáček and A. Procházka. Autoregressive Modelling in Rejection of Image Artefacts. In *13th International Conference on Process Control, Štrbské Pleso*. The Slovak Society of Cybernetics and Informatics, 2001.
- [9] S. D. Rane, G. Sapiro, and M. Bertalmio. Structure and Texture Filling-In of Missing Image Blocks in Wireless Transmission and Compression Applications. *IEEE Transactions on Image Processing*, 12(3):296–303, March 2003.
- [10] J. Romberg, H. Choi, and R. Baraniuk. Tree Structured Image Modeling. In *IEEE South-west Symposium on Image Analysis and Interpretation*, Austin, TX, U.S.A., April 2000.
- [11] R. Willett and R. Nowak. Platelets: A Multiscale Approach for Recovering Edges and Surfaces in Photon-Limited Medical Imaging. Technical report, Rice University, U.S.A., July 2003.

Mgr. Irena Šindelářová
Department of Econometrics
University of Economics, Prague
W. Churchill Sq. 4, 130 00 Prague 3
Phone.: (+420) 224 095 443, Fax: (+420) 224 095 432
E-mail: isin@vse.cz

Ing. Jiří Ptáček, Ph.D.
Prof. Ing. Aleš Procházka, CSc.
Department of Computing and Control Engineering
Institute of Chemical Technology, Prague
Technická 1905, 166 28 Prague 6
Phone: (+420) 224 352 970, Fax: (+420) 224 355 053
E-mail: J.Ptacek@ieee.org, A.Prochazka@ieee.org